Enzymatic degradation of low soluble compounds in monophasic water:solvent reactors. Kinetics and modelling of anthracene degradation by MnP

G. Eibes*, M. T. Moreira, G. Feijoo and J. M. Lema

Department of Chemical Engineering, School of Engineering, University of Santiago de Compostela, E-15782. Santiago de Compostela, Spain

Phone: +34-981563100 Ext.16740; e-mail: geibes@usc.es

Abstract

Polycyclic aromatic hydrocarbons (PAHs) are toxic compounds presenting low water solubility and high hydrophobicity, which greatly hampers their natural biodegradation. The enzymatic degradation of a model compound, anthracene, was evaluated in presence of a miscible solvent for an increased solubility. Manganese peroxidase, a ligninolytic enzyme from white-rot fungi, was used as biocatalyst in a medium containing acetone. The kinetic parameters of the enzymatic degradation of anthracene, obtained from fed-batch experiments, were applied to model the operation of a continuous reactor. Kinetics comprised a Michaelis-Menten equation, modified with an autocatalytic term, assumed to the effect of quinones acting as electron carriers, and a logistic function related to enzyme activity. The continuous reactor has been operated for 108 h, attaining a 90% of anthracene degradation, which demonstrated the feasibility of the system for its application in the removal of poorly-soluble compounds. The model of this reactor permitted to predict accurately anthracene degradation in different conditions, such as external addition of anthraquinone and different enzymatic activities.

Keywords: Enzyme bioreactors; Manganese peroxidase; Anthracene; Miscible solvent; Modelling

Introduction

Recalcitrant compounds are a major threat for the environment and in many cases they can constitute a health risk to humans and animals. In recent years there has been an increasing interest in the search of biological systems capable of degrading persistent pollutants. Among diverse recalcitrant compounds, polycyclic aromatic hydrocarbons (PAHs) present low solubility and great affinity to be adsorbed on the soil matrix and thus, their desorption from soil limits their availability for microbial biodegradation.

Enzymatic degradation is an attractive approach for the removal of recalcitrant compounds since it presents a series of advantages with respect to microbial treatment: shorter operational times, easier control and operation, non-sterile conditions, etc. The extracellular degrading system of white-rot fungi has permitted *in vitro* PAH biodegradation, this process is usually limited by the low solubility of the compounds in aqueous media (Field et al. 1995). The use of an organic solvent to desorb PAHs from the soil matrix can assist the degradative action of the enzymes (Field et al. 1996). The catalytic action of the ligninolytic enzyme manganese peroxidase (MnP) generates polar and water-soluble metabolites, such as quinones, which are susceptible for more readily biodegradation than the parent compounds (Meulenberg et al. 1997).

The economic feasibility of an enzymatic process is mostly influenced by the optimisation of the enzymatic reactor design and operation (Illanes and Wilson 2003), and particularly by the enzyme stability and its potential inactivation (Buchanan et al. 1998). Therefore, a comprehensive knowledge of enzyme kinetics is essential. Although Michaelis-Menten is the most widely used model to predict enzymatic reaction kinetics, in many processes enzymatic reactions do not follow the sequence of events, where free enzyme forms a single enzyme-substrate complex and further dissociates into free enzyme and product (Bailey and Ollis 1986; Segel 1993). That is the case of enzymatic

reactions carried out by MnP, where two different substrates are used during the catalytic cycle. Furthermore, enzyme deactivation may be significant and especially evident for an operation during an extended period of reaction, as may occur in the case of oxidation of barely biodegradable compounds by MnP (Eibes et al. 2005; Mielgo et al. 2003).

The objective of this work is to study the feasibility of enzymatic treatment of poorly-soluble and recalcitrant compounds in monophasic reactors. Anthracene, a tricyclic PAH, was selected as a model compound and acetone was added at 36% (v:v), which increased 140-fold anthracene solubility in aqueous media. Acetone at concentrations below 10% does not substantially inhibit aerobic or anaerobic sludges (Eibes, 2007). Regarding the biodegradability, there are studies with several different strains bacteria (aerobic and anaerobic) which demonstrated that acetone is readily biodegradable (Platen and Schink 1989; Price et al. 1974).

Different configurations of the reactor were also taken into account to determine the influence of the different factors affecting process kinetics. The work will also consider the development of a model describing substrate conversion, product generation and enzyme deactivation.

Materials and methods

Chemicals

Anthracene and anthraquinone were obtained from Janssen Chimica (95-99% purity). Acetone was obtained from Panreac (chemical purity). H_2O_2 (30% v:v), sodium malonate and manganese sulphate were from Sigma-Aldrich.

MnP production

MnP was obtained from *Bjerkandera* sp. BOS55 (ATCC 90940). The fungus was grown in a 10-L fermenter BIOSTAT®E B. Braun-Biotech International (Melsungen,

Germany), on skimmed cheese whey medium (Feijoo et al. 1999; Moreira et al. 2001). Once the peak production of MnP was detected, the fermentation was stopped by decreasing temperature and the extracellular liquid was vacuum filtered. High molecular weight polysaccharides were precipitated by freeze-thawing and removed by filtration. Crude enzyme was concentrated by ultrafiltration using a 10 kDa cut-off type YM-10 membrane (Amicon), and was then centrifuged for 10 min at 20,000×*g*. Neither Lignin peroxidase nor Laccase activities were detected in any of the separated fractions during the procedure.

Analytical techniques

MnP activity was determined spectrophotometrically (Cecil CE 7200, UK) at 30ºC and 468 nm as described by Field et al (1992). The method is based on the oxidation of 2,6-dimethoxyphenol (2,6-DMP) by MnP system to form a quinone dimer. The molar extinction coefficient is 49600 M^{-1} cm^{-1}. MnP assays were carried out with 200 µL sodium malonate (250 mM, pH 4.5), 50 µL 2,6-DMP (20 mM), 50 µL $MnSO_4$ (20 mM), 50 µL of the sample whose MnP activity is to be determined and 550 µL water. The reaction was started by the addition of 100 µL H_2O_2 (4 mM), ending up with a volume of 1 mL. One unit of activity was considered as the amount of enzyme which oxidizes one µmol per min.

Anthracene and anthraquinone were analyzed by a HP 1090 HPLC, equipped with a diode array detector monitoring the absorbance at 254 nm, a 4.6 x 200 mm Spherisorb ODS2 reverse phase column (5 µm; Waters) and a HP ChemStation data processor. The injection volume was set at 10 µL and the isocratic eluent (80% acetonitrile and 20% water) was pumped at a rate of 1 mL min^{-1}.

Fed-batch reactors

Oxidation of anthracene was carried out in 100-mL Erlenmeyer flasks sealed with

Teflon plugs, with magnetic stirring at room temperature (about 22ºC). The reaction mixture (50 mL) consisted of acetone 36% (v:v), anthracene (28 μM), MnP (200 U L^{-1}), Mn^{2+} (20 μM), malonic acid (20 mM) at pH 4.5 and anthraquinone (14 μM) when indicated. The reaction started with the continuous addition of 5 μmol L^{-1} min^{-1} of H_2O_2 supplied by a peristaltic pump running at 20 μL min^{-1}. The dilution effect caused by H_2O_2 addition was considered to calculate accurate concentrations in the reactor. MnP (2.5 mL of enzymatic crude) was periodically added in the reactor. Samples were withdrawn at regular intervals to determine anthracene and anthraquinone concentrations by HPLC and the evolution of MnP activity was spectrophotometrically determined. Experiments were run in duplicate. To verify that degradation took place only due to enzymatic oxidation, controls were run in parallel using boiled MnP. No change in anthracene concentration after 6-8 h of incubation was observed in any controls (data not shown).

Semi-continuous reactor

Oxidation of anthracene was carried out in 250-mL Erlenmeyer flasks sealed with Teflon plugs, with magnetic stirring at room temperature (about 22ºC). The volume of the reactor was 150 mL and the hydraulic retention time (HRT) was 11.5 h. All reagents were added continuously but for MnP, which was added once enzymatic activity reached zero in the reactor. Concentrations of the different compounds in the reactor at the beginning of the reaction were as follows: anthracene 28 μM; acetone 36% (v:v); sodium malonate 20 mM; Mn^{2+} 20 μM and MnP 200 U L^{-1}. The process was initiated by the addition of two solutions: i) A solution containing anthracene 34 μM, acetone 42%, Mn^{2+} 23.4 μM and sodium malonate 23.4 mM (pH 4.5), was pumped at 10 mL h^{-1} using a high precision pump P-500 (Pharmacia) with Teflon tubes to avoid anthracene adsorption; and ii) A solution of H_2O_2: 5 μmol $L^{-1}\cdot min^{-1}$ was pumped at 2 mL h^{-1} using

a Masterflex peristaltic pump (Cole Palmer). This H_2O_2 solution was stored in a cool box and periodically changed. During the time course of the experiments, MnP pulses were regularly added to restore enzyme concentrations to levels around 200 U L^{-1}. A third pump was used for the discharge of the effluent. Samples were obtained directly from the Erlenmeyer flask.

Continuous reactor

Continuous oxidation of anthracene was carried out in a reactor working under identical conditions to those of semi-continuous reactor. In this case, three solutions were added: i) A solution containing anthracene 41 μM, acetone 52%, Mn^{2+} 28.9 μM and sodium malonate 28.9 mM (pH 4.5) was pumped at 9 mL h^{-1} using a high precision pump P-500 (Pharmacia) with Teflon tubes to avoid anthracene adsorption; ii) A solution of H_2O_2 5 μmol $L^{-1}\cdot min^{-1}$ was pumped at 2.5 mL h^{-1} through a Masterflex peristaltic pump (Cole Palmer) and iii) A solution containing different MnP activities: 3350, 4630 and 7500 U L^{-1} was used to pump MnP at different addition rates: 36, 50 and 75 U $L^{-1}\cdot h^{-1}$, respectively. MnP crude was stored in a cool box to minimise thermal inactivation. A fourth pump was used for the discharge of the effluent. Samples were obtained directly from the Erlenmeyer flask.

Method of numerical integration

A software package using an algorithm based on a Runge-Kutta formula (the Dormand-Prince pair) was used to solve the set of nonlinear ordinary differential equations. It is a one-step solver: in computing $y(t_n)$, it needs only the solution at the immediately preceding time point, $y(t_{n-1})$.

Results and discussion

Batch experiments: The kinetic model

As previously stated, the oxidation mechanism of MnP is a multi-step process, comprising different reactions at different rates. Although the enzyme's first substrate is usually considered the substrate of the reaction, the slowest step of the degradation will limit the apparent kinetics of the whole process. In the present work, the real oxidizing agent of anthracene is the Mn^{3+}-malonate complex. The formation of this complex is followed by oxidation of MnP to MnPI by H_2O_2 and reduction by Mn^{2+} of MnPI and MnPII to the initial state (See catalytic cycle in Figure 1). An excess of H_2O_2 may lead to partial or total irreversible inactivation of the enzyme. The first oxidation, reductions to produce Mn^{3+} and formation of the malonate complex are rapid reactions, as shown by their kinetic constants (Wariishi et al. 1989; Wariishi et al. 1992). When the enzymatic reaction is faster than the oxidation of the final recalcitrant compounds, the latter reaction turns out to be the limiting step in the degradation process. Therefore, the overall kinetics will match up with the degradation kinetics of the final substrate, in this case, anthracene.

A first experiment was carried out maintaining MnP activity in the range around 100 to 200 U L^{-1}, because lower enzymatic activities have been shown to greatly limit degradation extent (Mielgo et al. 2003). Figure 2A shows the time course profile of an experiment performed during 7 h with enzyme pulses added after 1.5 h and 5.5 h.

As a preliminary approach, first-order and Michaelis-Menten kinetics were considered; the former was taken into account due to the very low concentration of the final substrate (around 28 μM of anthracene). Significant discrepancies relative to experimental data are evident in Figure 2B, where experimental, first-order and Michaelis Menten degradation rates were plotted. The kinetics constants considered to

plot the models were those obtained from the integrated first-order equation (k_{cat}=0.39 h^{-1} and r^2=0.97) and the Eadie-Hotstee linearisation (r_m=7.02 μM h^{-1}, K_M=8.47 μM and r^2=0.62). In the case of first-order kinetics the decrease of oxidation rates would be very rapid during the first hours whereas for Michaelis-Menten kinetics lower degradation rates than first order would be observed. The experimental degradation rates followed a different pattern for the first 2 h, where a bell-shaped curve was observed. The first increase and further stabilisation of the degradation rate observed in the experiment could be explained by the presence of an activating agent, which may first increase degradation rates and subsequently balance the decrease of anthracene concentration.

Quinones have been described to play a role as electron carriers in redox processes (Kudlich et al. 1997; Méndez-Paz et al. 2005; van der Zee et al. 2000). Considering that anthraquinone is the main metabolite produced in the anthracene degradation by MnP (Eibes et al. 2006), a possible explanation of the reaction behaviour could arise from the autocatalytic effect of the products formed, as described in Figure 3. Therefore a modified Michaelis-Menten equation including an auto-catalytic effect caused by the reaction products was considered as the model basis (equation 1):

$$r_S = -\frac{r_m \cdot S}{K_M + S} \cdot (a + b \cdot P) \qquad \text{(eq 1)}$$

Considering that products refer not only to anthraquinone but also other intermediates formed during degradation (anthrone, dihydroxyanthrone), the rate of substrate formation in a batch experiment is given by:

$$\frac{dS}{dt} = -\frac{r_m \cdot S}{K_M + S} \cdot \left[a + b \cdot \left(P_0 + S_0 - S \right) \right] \qquad \text{(eq 2)}$$

In order to validate this approach, an experiment where anthraquinone was added at the beginning of the reaction (14 μM), was carried out. Degradation rates were higher in this experiment, since 90% of anthracene had been degraded after 5 h whereas

in the first experiment without anthraquinone at the beginning, only 78% of degradation was attained (Figure 4). The kinetic constants r_m, K_M, *a* and *b* were estimated by using the method of least squares for the two experiments (with and without anthraquinone) and their duplicates. The sequence of the program utilised for calculating the parameters is shown in Figure 5.

Continuous reactor: Effect of the enzymatic activity

The effect of different MnP stationary activities on the degradation of anthracene was evaluated in a continuous reactor. As the enzyme is subjected to inactivation and washout, a continuous flow of MnP was necessary to maintain a stationary activity value. Three different MnP addition rates were studied: I) 36, III) 50 and IV) 75 U $L^{-1}h^{-1}$ (Figure 6). In the first stage, steady state was achieved after 24 h (11 μM of anthracene) whereas the stabilisation of enzymatic activity (around 30 U L^{-1}) was reached in 6 h. During stage II, there was no MnP addition, which led to anthracene accumulation in the reactor. In the third stage a failure of enzyme dosage (around 66 h) was detected, reaching again the steady state after 5 h (49 U L^{-1} and 8.5 μM). In stage IV, as the enzymatic flow increased, MnP activity also increased in the reactor (around 76 U L^{-1}), leading to the lowest stationary concentration of anthracene (4 μM).

Data showed that MnP activity clearly affects the extent of anthracene degradation: the higher the enzymatic activity inside the reactor, the lower anthracene concentration (Table I). The effect of the enzymatic activity on anthracene degradation was included in the kinetic equation by means of a function, Y(E). Mass balances of anthracene and products in the continuous reactor are given by equations 3 and 4, and MnP inactivation was evaluated as first-order decay (included in equation 5) as commonly described in literature (Baldascini and Janssen 2005; Illanes and Wilson 2003; Reading and Aust 2000).

$$\frac{dS}{dt} = \frac{Q_i}{V_R} \cdot S_i - \frac{1}{\tau} \cdot S - y(E) \cdot \frac{r_m \cdot S}{k_m + S} \cdot (a + b \cdot P) \quad \text{(eq 3)}$$

$$\frac{dP}{dt} = -\frac{1}{\tau} \cdot P + y(E) \cdot \frac{r_m \cdot S}{k_m + S} \cdot (a + b \cdot P) \quad \text{(eq 4)}$$

$$\frac{dE}{dt} = \frac{Q_e}{V_R} \cdot E_i - \frac{1}{\tau} \cdot E - k_d \cdot E \quad \text{(eq 5)}$$

By applying steady state conditions for substrate and products in equations 3 and 4 (dS dt^{-1}=dP dt^{-1}=0), and using stationary values of S and E, the stationary values of Y(E) and P were obtained for each steady state condition (Table I).

The correlation of Y(E) was formulated considering two additional conditions: a) when no enzyme is present in the reactor, no enzymatic reaction took place, i.e. Y(0)=0; and b) enzymatic activities above 200 U L^{-1} do not enhance substrate degradation (Mielgo et al. 2003), therefore Y(200)=1 and Y(300)=1. A logistic equation (dose response) with 3 parameters fulfilled all conditions (Equation 6; Figure 7).

$$y(E) = \frac{c}{1 + \left(\frac{E}{d}\right)^e} \quad \text{(eq 6)}$$

Where parameter *c* is the maximum value of the function; *d* is the transition centre; *e* is negative for ascending functions and represents the rate of rise.

To determine the time course of enzymatic activity, the inactivation of the enzyme should be considered and it was calculated assuming a first-order inactivation model. k_d values were obtained from experimental data of fed-batch experiments (in absence or presence of anthraquinone) and continuous reactor (Table II). Two values of k_d were obtained in fed-batch experiments, suggesting a sequential two-step process, which has been already described for thermal inactivation kinetics of MnP (Reading and Aust 2000; Sutherland and Aust 1996). Fed-batch experimental data were processed together with continuous experimental data to obtain the parameters of kinetics comprising a

modified Michaelis-Menten and an enzymatic function (Table III). Modelling of fed-batch experiments, using the complete kinetic equation, is shown in Figure 8 for experiments in absence or presence of external anthraquinone. In the continuous reactor, the numerical integration in the four periods of the operation gave the fitting shown in Figure 6.

Semicontinuous reactor: Model validation

In order to validate the kinetic equation proposed including all the terms (substrate, enzyme and products) as well as model parameters, a semi-continuous reactor was modelled. In the operation of this reactor all reagents were continuously added (HRT = 11.5 h) except MnP, which was supplied (at different concentrations) when the activity in the reactor was nearly zero. The equations of the model are given by:

$$\frac{dS}{dt} = \frac{Q_i}{V_R} \cdot S_i - \frac{1}{\tau} \cdot S - \frac{r_m \cdot S}{K_M + S} \cdot (a + b \cdot P) \cdot \left(\frac{c}{1 + \left(E/d \right)^e} \right) \quad \text{(eq 7)}$$

$$\frac{dP}{dt} = -\frac{1}{\tau} \cdot P + \frac{r_m \cdot S}{K_M + S} \cdot (a + b \cdot P) \cdot \left(\frac{c}{1 + \left(E/d \right)^e} \right) \quad \text{(eq 8)}$$

$$\frac{dE}{dt} = -\frac{1}{\tau} \cdot E - k_d \cdot E \quad \text{(eq 9)}$$

After each MnP pulse, the substrate and product concentrations were corrected according to the dilution caused by the enzyme addition. The enzymatic decay constant obtained from experimental data was k_d=0.25 h^{-1}, the lowest value observed in the different experiments (Table II). The divergences observed on enzymatic inactivation could be attributed to the different origin of the enzyme crude, produced in different fermentations, with slight different characteristics.

Figure 9 shows anthracene and MnP activity profile during the 104 h of operation. The higher discrepancies between the model and experimental data occurred during the period where the adjustment of enzymatic activity to a first-order decay

model was less satisfactory, from 42 to 78 h, and thus indicating that the knowledge of enzymatic decay kinetics is critical for the overall model of the process.

Conclusions

The use of enzymatic reactors containing adequate concentrations of miscible solvents represents a valuable tool for the degradation of compounds with low water solubility and barely biodegradable. In the present work, acetone at 36% v:v enabled the efficient degradation of anthracene by MnP as a result of increased substrate availability and moderate enzyme inactivation. The potential of this system has been proved in three different configurations of monophasic solvent:water reactors: fed-batch, semi-continuous and continuous reactors.

Anthraquinone, the main product of the reaction, has been shown to produce an autocatalytic effect, accelerating the degradation rate of anthracene. Processes where quinones are involved should therefore consider their positive influence on the enzymatic catalysis, acting as electron carriers.

The kinetic model proposed in this work is based on the three main components of the reaction: substrate, products and enzyme. A modified Michaelis-Menten equation including an autocatalytic effect attributed to the oxidation products and a logistic function related to enzyme activity is used to predict anthracene and MnP time-course profiles in the different reactor configurations. Enzyme activity should be maintained in a specific range to ensure an efficient and economical operation of the enzymatic reactor; the degradation extent not being enhanced above 200 U L^{-1}, whereas low enzymatic activities (below 100 U L^{-1}) greatly limit the oxidation.

The enzymatic reactor presented in this work appears as an attractive technology for the removal of poorly-soluble compounds, which has to be further optimised and

tested on a larger scale. Recovering the enzyme and increasing the efficiency (in terms of mass of pollutant degraded/units of enzyme inactivated) as well as improving the reliability in continuous reactors by implementing control systems are some of the goals to be attained in a near future.

Acknowledgments

This work was funded by Xunta de Galicia (PGIDIT06P- XIB265088PR) and Spanish Ministry of Education and Science (CICYT-CTQ2007-66788/PPQ). Support given to Gemma Eibes from the Spanish Ministry of Science and Technology (BES-2002-2809) is also greatly appreciated.

Nomenclature

a	1^{est} catalytic constant
b	2^{nd} catalytic constant (μM^{-1})
c	3^{rd} catalytic constant
d	4^{th} catalytic constant
e	5^{th} catalytic constant
E	Enzymatic activity in the reactor (U L^{-1})
E_0	Initial enzymatic activity in the reactor (U L^{-1})
E_i	Enzymatic activity in the input flow (U L^{-1})
k_d	Decay constant (h^{-1})
K_M	Michaelis-Menten constant (μM)
P	Concentration of products in the reactor (μM)
P_0	Initial concentration of products in the reactors (μM)
Qe	Input flow of the enzyme solution (L h^{-1})

Q_i	Input flow of the substrate solution (L h^{-1})
r_m	Maximum rate (μM h^{-1})
S	Concentration of anthracene in the reactor (μM)
S_0	Initial concentration of anthracene in the reactor (μM)
S_i	Concentration of anthracene in the input flow (μM)
t	Time (h)
t_0	Initial time (h)
V_R	Volume of the reactor (L)
Y(E)	Function dependent on enzymatic activity (dimensionless)
τ	Hydraulic retention time (h)

References

Bailey JE, Ollis DF. 1986. Biochemical engineering fundamentals. New York: McGraw-Hill Publishing Co. 928 p.

Baldascini H, Janssen DB. 2005. Interfacial inactivation of epoxide hydrolase in a two-liquid-phase system. Enzyme Microb Technol 36:285-293.

Buchanan ID, Nicell JA, Wagner M. 1998. Reactor models for horseradish peroxidase-catalyzed aromatic removal. J Environ Eng 124:794-802.

Eibes G. 2007. Enzymatic degradation of polycyclic aromatic hydrocarbons (PAHs) by manganese peroxidase in reactors containing organic solvents. Ph.D. thesis, University of Santiago de Compostela, Santiago de Compostela.

Eibes G, Cajthaml T, Moreira MT, Feijoo G, Lema JM. 2006. Enzymatic degradation of anthracene, dibenzothiophene and pyrene by manganese peroxidase in media containing acetone. Chemosphere 64:408-414.

Eibes G, Lu Chau T, Feijoo G, Moreira MT, Lema JM. 2005. Complete degradation of anthracene by Manganese Peroxidase in organic solvent mixtures. . Enzyme Microb Technol 37:365-372.

Feijoo G, Moreira MT, Roca E, Lema JM. 1999. Use of cheese whey as a substrate to produce manganese peroxidase by *Bjerkandera* sp BOS55. J Ind Microbiol Biotechnol 23:86-90.

Field JA, Baten H, Boelsma F, Rulkens WH. 1996. Biological elimination of polycyclic aromatic hydrocarbons in solvent extracts of polluted soil by the white rot fungus, *Bjerkandera* sp strain BOS55. Environ Technol 17:317-323.

Field JA, Boelsma F, Baten H, Rulkens WH. 1995. Oxidation of anthracene in water/solvent mixtures by the white- rot fungus, *Bjerkandera* sp strain BOS55. Appl Microbiol Biotechnol 44:234-240.

Field JA, de Jong E, Feijoo G, de Bont JAM. 1992. Biodegradation of polycyclic aromatic hydrocarbons by new isolates of white-rot fungi. Appl Environ Microbiol 58:2219-2226.

Illanes A, Wilson L. 2003. Enzyme reactor design under thermal inactivation. Crit Rev Biotechnol 23:61-93.

Kudlich M, Keck A, Klein J, Stolz A. 1997. Localization of the enzyme system involved in anaerobic reduction of azo dyes by *Sphingomonas* sp. strain BN6 and effect of artificial redox mediators on the rate of azo dye reduction. Appl Environ Microbiol 63:3691-3694.

Méndez-Paz D, Omil F, Lema JM. 2005. Anaerobic treatment of azo dye Acid Orange 7 under batch conditions. Enzyme Microb Technol 36:264-272.

Meulenberg R, Rijnaarts HHM, Doddema HJ, Field JA. 1997. Partially oxidized polycyclic aromatic hydrocarbons show an increased bioavailability and biodegradability. FEMS Microbiol Lett 152:45-49.

Mielgo I, López C, Moreira MT, Feijoo G, Lema JM. 2003. Oxidative degradation of azo dyes by manganese peroxidase under optimized conditions. Biotechnol Prog 19:325-331.

Moreira MT, Palma C, Mielgo I, Feijoo G, Lema JM. 2001. In vitro degradation of a polymeric dye (Poly R-478) by manganese peroxidase. Biotechnol Bioeng 75:362-368.

Platen H, Schink B 1989. Anaerobic degradation of acetone and higher ketones via carboxylation by newly isolated denitrifying bacteria. J Gen Microbiol 135:883-891.

Price KS, Waggy GT, Conway RA 1974. Brine shrimp bioassay and seawater BOD of petrochemicals. J Water Pollut Control Fed 46:63-77.

Reading NS, Aust SD. 2000. Engineering a disulfide bond in recombinant manganese peroxidase results in increased thermostability. Biotechnol Prog 16:326-333.

Segel IH. 1993. Enzyme kinetics: behavior and analysis of rapid equilibrium and steady-state enzyme systems. New York: Wiley. 984 p.

Sutherland GRJ, Aust SD 1996. The effects of calcium on the thermal stability and activity of manganese peroxidase. Arch Biochem Biophys 332:128-134.

van der Zee FP, Lettinga G, Field JA. 2000. The role of (auto)catalysis in the mechanism of an anaerobic azo reduction. Water Sci Technol 42:301-308.

Wariishi H, Dunford HB, MacDonald ID, Gold MH. 1989. Manganese peroxidase from the lignin-degrading basidiomycete *Phanerochaete chrysosporium*. Transient state kinetics and reaction mechanism. J Biol Chem 264:3335-3340.

Wariishi H, Valli K, Gold MH. 1992. Manganese(II) oxidation by manganese peroxidase from the basidiomycete *Phanerochaete chrysosporium* - kinetic mechanism and role of chelators. J Biol Chem 267:23688-23695.

Table I. Stationary values of the enzymatic function at the different stages of the continuous reactor operation

Stage	E* (U L^{-1})	S* (μM)	P† (μM)	Y† (E)
I	30	11.0	17.34	0.311
III	49	8.5	19.84	0.396
IV	76	4.0	24.34	0.753

* Experimental data (Figure 7)

† Calculated from the set of equations 3 and 4 at steady state conditions

Table II. Values of inactivation decay constants in fed-batch reactors in absence (FB 1) and presence (FB 2) of external anthraquinone, continuous reactor (CR) and semicontinuous reactor (SCR)

	k_{d1}	k_{d2}	r^2
FB 1	0.66 ± 0.17	0.42 ± 0.08	0.97
FB 2	0.86 ± 0.36	0.62 ± 0.11	0.99
CR	1.00		0.73
SCR	0.25		0.73

Table III. Values of kinetic parameters (modified Michaelis-Menten r^2 0.998; enzymatic function r^2 0.996)

r_m (μM h^{-1})	k_M (μM)	a	b (μM^{-1})	c	d	e
13.30	10.99	0.572	0.009	1.07	54.42	-1.82

CAPTIONS TO FIGURES

Figure 1 Catalytic cycle of MnP

Figure 2 (A) Time course of anthracene (■), anthraquinone (▲) and MnP enzymatic activity (○) during MnP fed-batch experiment (B) Experimental degradation rates (■) compared to those obtained using first-order (— · —) and Michaelis-Menten (—) models

Figure 3 Autocatalytic mechanism of the anthracene oxidation by MnP

Figure 4 Modelling of anthracene using Michaelis-Menten and autocatalytic kinetics in the MnP fed-batch reactors in absence (□) and in presence of anthraquinone (○) in the initiation of the reaction. Kinetic parameters: r_m: 13.574 μM h^{-1}; K_M=14.72 μM; a=0.549; b=0.008 μM^{-1} (r^2=0.995)

Figure 5 Sequence scheme for obtaining kinetic parameters

Figure 6 Fitted (—) and experimental data of anthracene (■) and MnP enzymatic activity (○) at different addition rates of MnP: I) 36 U L^{-1} h^{-1}, II) no addition of MnP, III) 50 U L^{-1} h^{-1} and IV) 75 U L^{-1} h^{-1}

Figure 7 Function defining the effect of enzymatic activity on the degradation of anthracene (eq. 6). Kinetic parameters are shown in Table III

Figure 8 Modelling of first-order inactivation of enzymatic activity (△) and anthracene degradation (○) using Michaelis-Menten, autocatalytic kinetics and an enzymatic function in the MnP fed-batch reactors in absence (A) and in presence of external anthraquinone (B). Kinetic parameters are shown in Table III

Figure 9 Fitted (—) and experimental data of: A) anthracene disappearance (■) and B) MnP enzymatic activity (○) during semi-continuous experiment

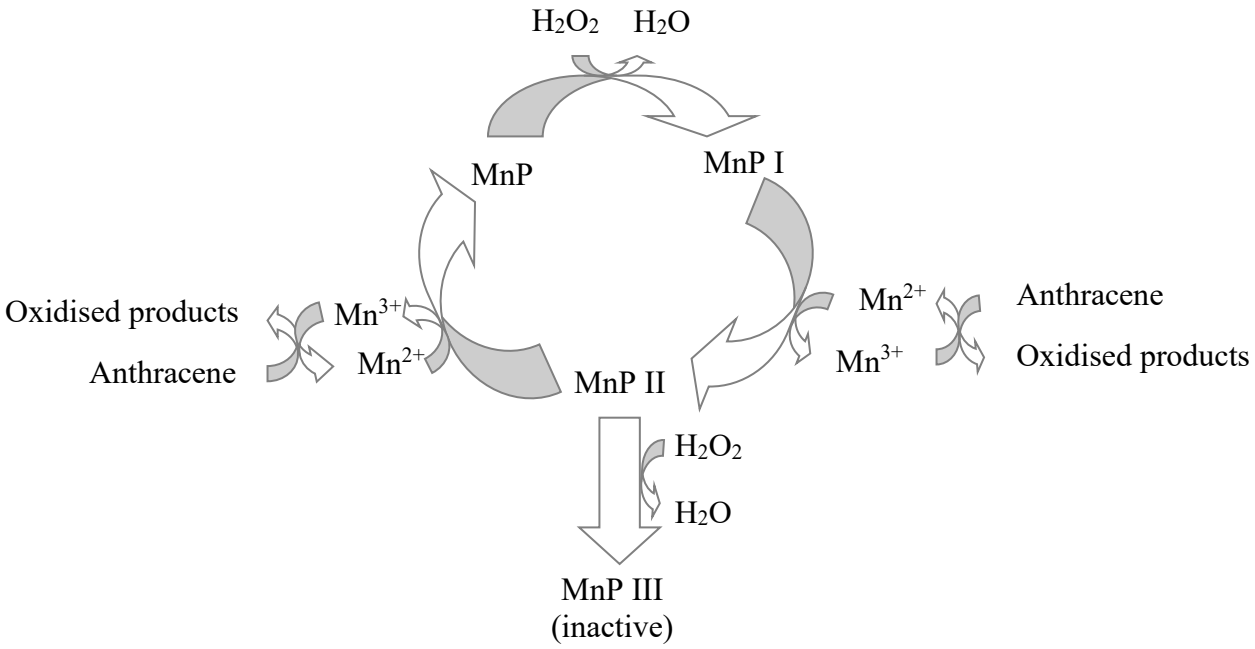
H2O2
H2O
MnP
MnP I
Oxidised products
Anthracene
Mn3+
Mn2+
Mn2+
Mn3+
Anthracene
Oxidised products
MnP II
H2O2
H2O
MnP III
(inactive)

Figure 1

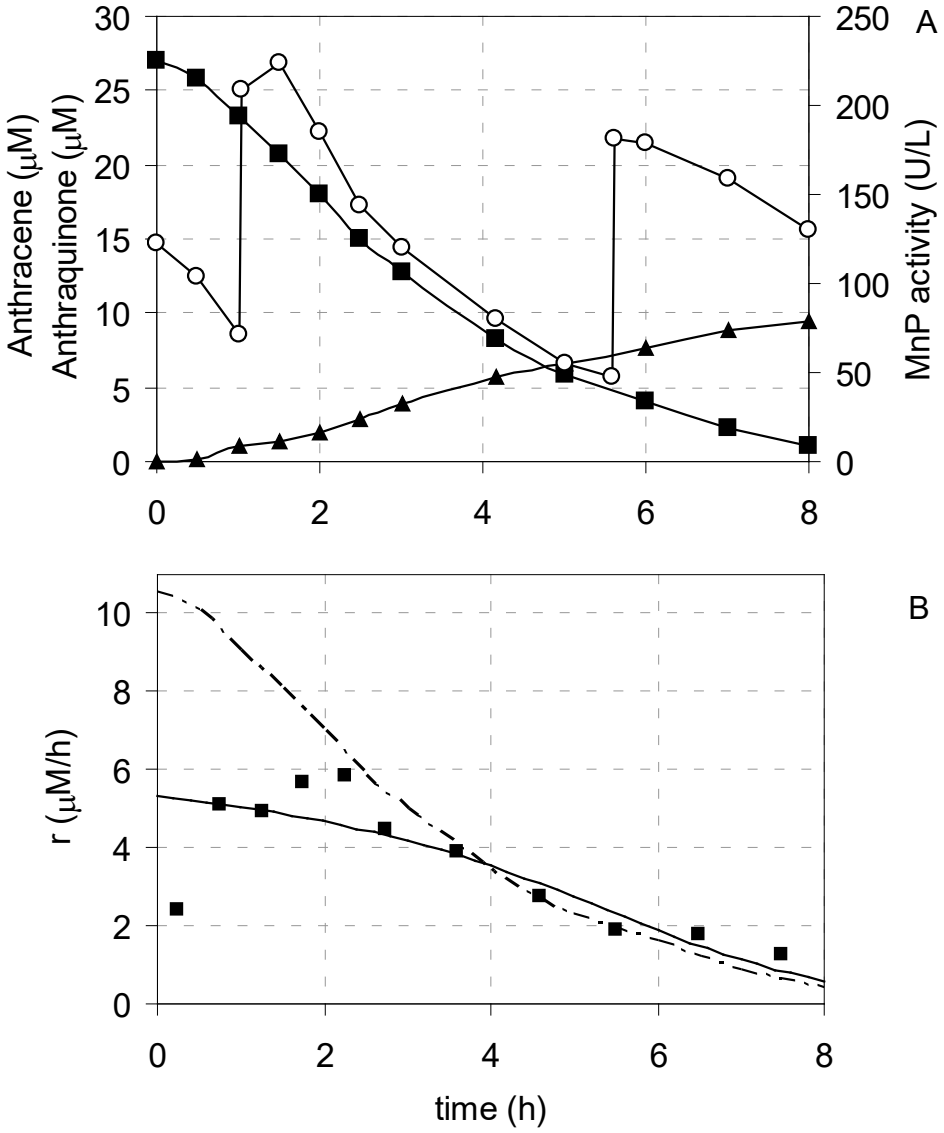
A
Anthracene (μM)
Anthraquinone (μM)
MnP activity (U/L)
B
r (μM/h)
time (h)

Figure 2

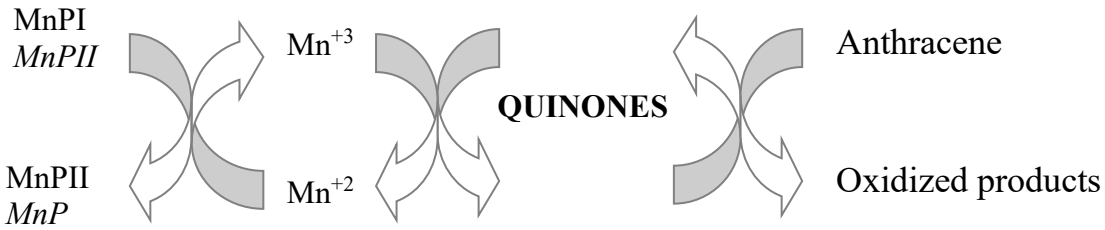

Figure 3

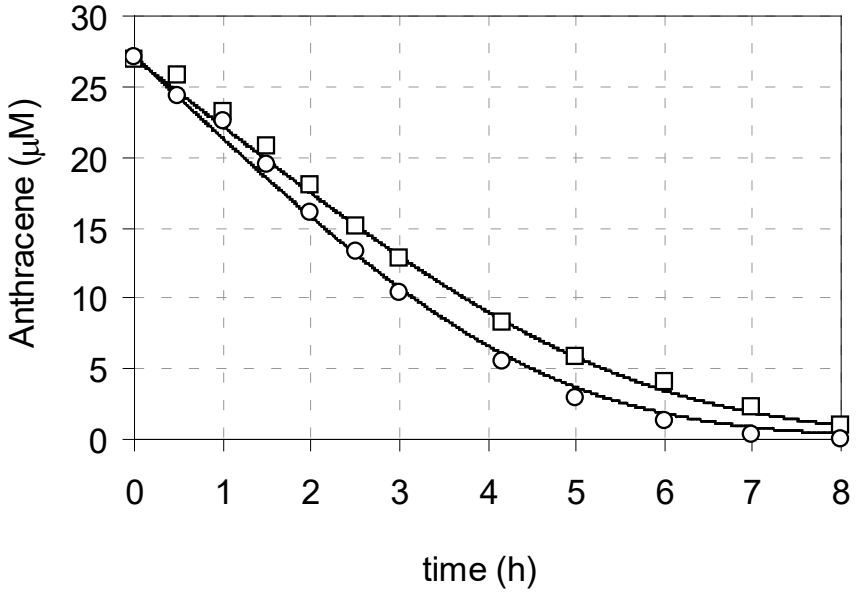

Figure 4

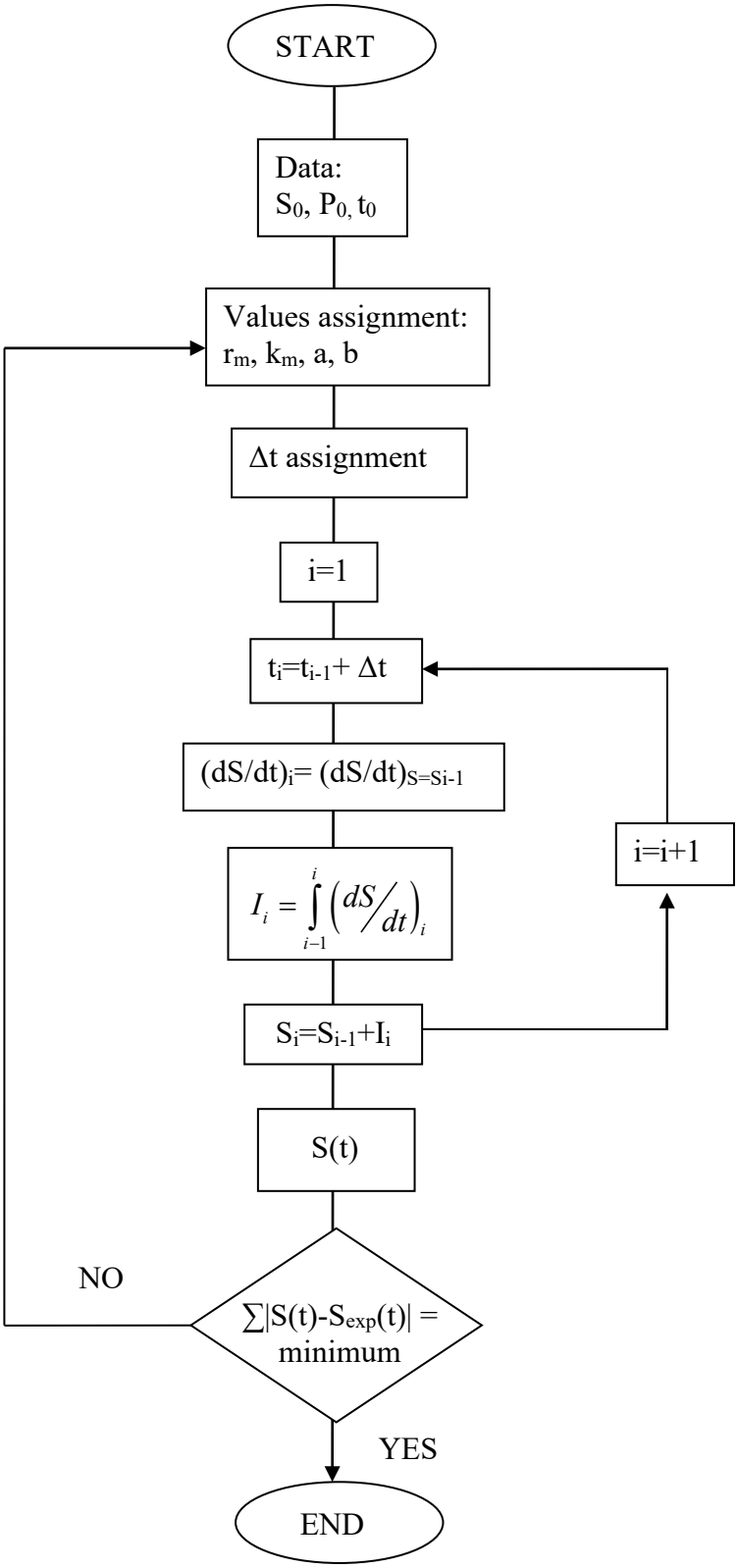
START
Data:
S_0, $P_{0,}$ t_0
Values assignment:
r_m, k_m, a, b
Δt assignment
i=1
$t_i=t_{i-1}+\Delta t$
$(dS/dt)_i=(dS/dt)_{S=Si-1}$
$I_i=\int_{i-1}^{i}\left(dS/dt\right)_i$
$S_i=S_{i-1}+I_i$
i=i+1
S(t)
NO
$\sum|S(t)-S_{exp}(t)|$ = minimum
YES
END

Figure 5

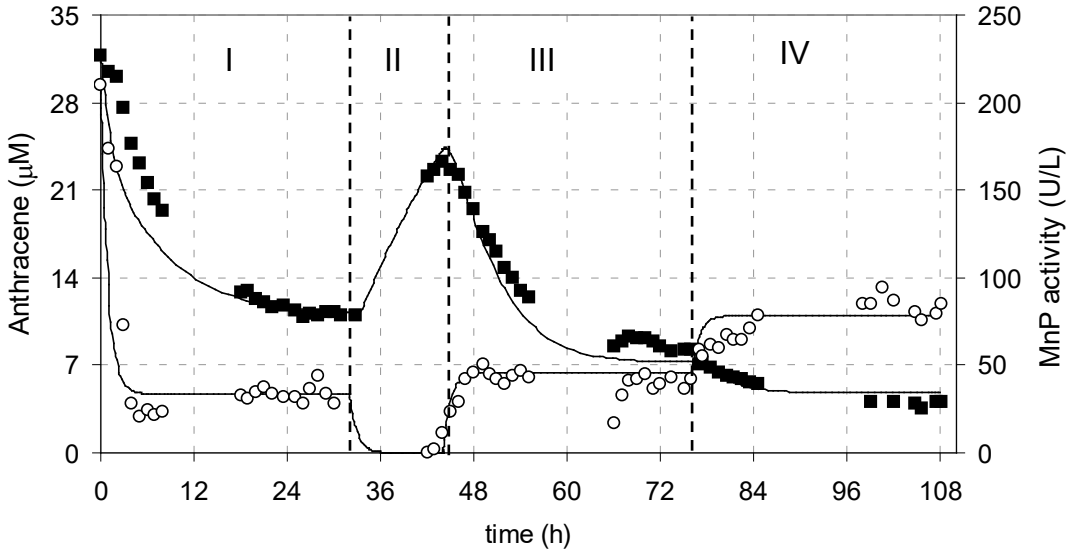
35
28
21
14
7
0
250
200
150
100
50
0
I
II
III
IV
0
12
24
36
48
60
72
84
96
108
time (h)
Anthracene (μM)
MnP activity (U/L)

Figure 6

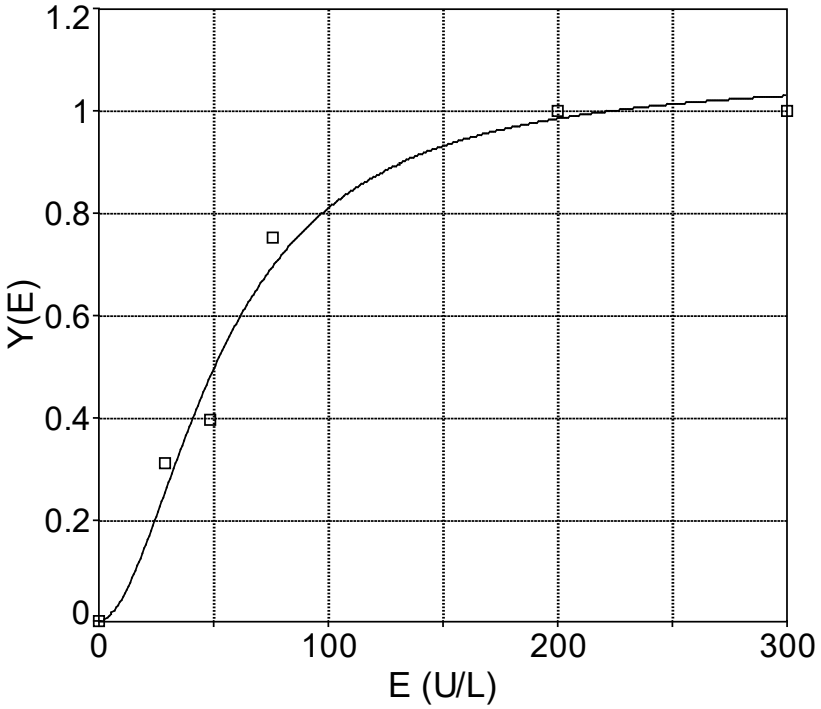

Figure 7

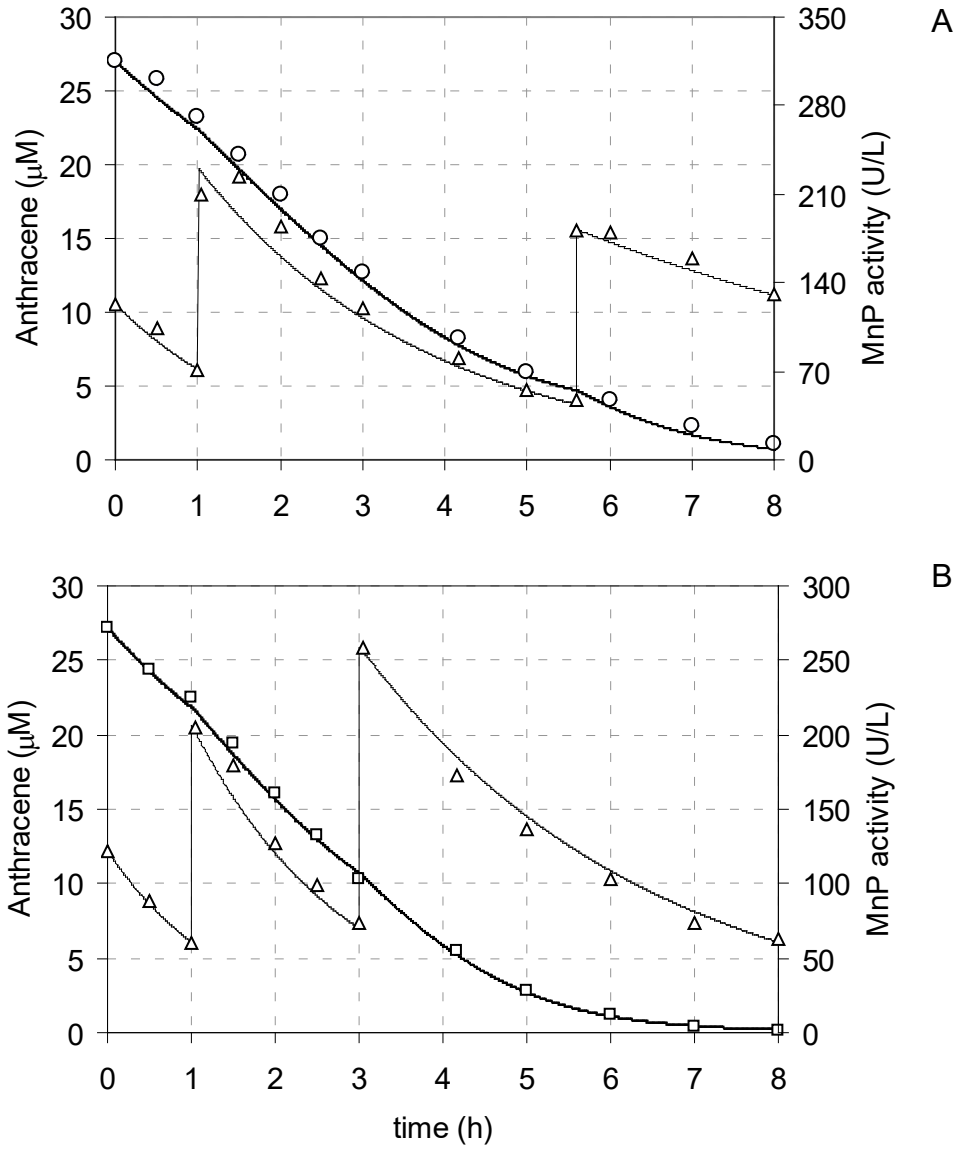
A
B
Anthracene (μM)
MnP activity (U/L)
time (h)
0
5
10
15
20
25
30
0
70
140
210
280
350
50
100
150
200
250
300
0
1
2
3
4
5
6
7
8

Figure 8

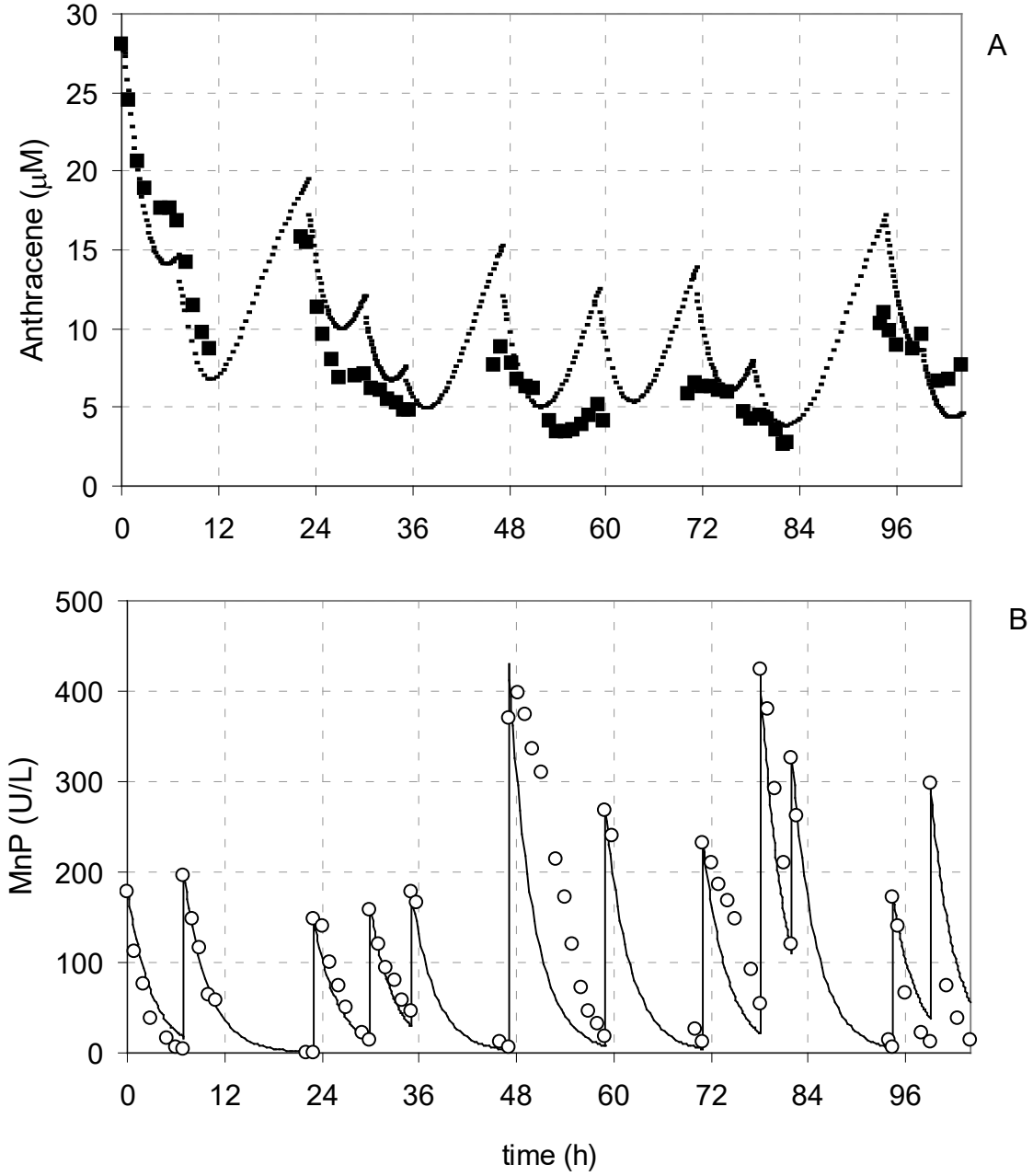
A
Anthracene (μM)
30
25
20
15
10
5
0
0
12
24
36
48
60
72
84
96
B
MnP (U/L)
500
400
300
200
100
0
0
12
24
36
48
60
72
84
96
time (h)

Figure 9